

Coating thermal noise investigation for KAGRA

Yukino Mori,^a Yota Nakayama,^a Takafumi Ushiba^b and Kazuhiro Yamamoto^{a,*}

^a*Department of Physics, Faculty of Science, University of Toyama,
Toyama, Toyama, Japan, 930-8555*

^b*Institute for Cosmic Ray Research, KAGRA Observatory, The University of Tokyo
Kamioka-cho, Hida City, Gifu 506-1205, Japan*

E-mail: yamamoto@sci.u-toyama.ac.jp

Gravitational wave astronomy is an emerging field in astronomy and astrophysics. For proper investigation and research in this field, the noise in the interferometers used as gravitational wave detectors must be reduced. Thermal noise caused by mechanical loss in the reflective coating on the mirrors is a fundamental source of noise. The cryogenic technique is a noise reduction method adopted by KAGRA (Kamioka, Japan) and the Einstein Telescope (to be constructed in Europe). However, further thermal noise reduction is required. For this purpose, an apparatus for measuring the mechanical loss of the coating at cryogenic temperatures must be developed.

Such an apparatus was prepared at University of Toyama, Japan. The apparatus was cooled using liquid nitrogen and helium. The losses of the sample disks with and without the coating were measured. The mechanical loss in the coating and the thermal noise were derived from the difference between the losses of the sample disks with and without the coating. This apparatus was then used to investigate conventional coatings; and this apparatus is expected to be used in coatings in the future. The outline and important details of the apparatus are provided in this article.

38th International Cosmic Ray Conference (ICRC2023)
26 July - 3 August, 2023
Nagoya, Japan



*Speaker

1. Introduction

Over 100 years ago, Einstein discovered gravitational waves from the study of the theory of general relativity. This is the space-time ripple of space time, whose velocity is the same as the speed of light. In 2015, the gravitational wave was detected directly using laser interferometers [1]. This marked the birth of gravitational wave astronomy and revealed many aspects of the Universe, such as black hole binaries. Between 2015 and 2020, the LIGO and Virgo interferometers detected approximately 100 events [2]. To conduct more in-depth investigation of the Universe, noise reduction of interferometric gravitational wave detectors is necessary.

Thermal noise from the internal elastic modes of mirrors is a fundamental noise [3], which is caused by mechanical loss in the reflective coating of the mirrors [4, 5]. The noise amplitude is proportional to the square root of the product of the mechanical loss in the coating and mirror temperature. LIGO and Virgo were used to investigate methods to reduce the mechanical loss of the coating. KAGRA [6] (Kamioka, Japan) adopts another technique to reduce thermal noise, that is, cryogenics. The mirror temperature is approximately 20 K. To evaluate the coating thermal noise amplitude at the cryogenic temperature, the mechanical loss of the coating must be measured at low temperatures because the loss may depend on the temperature. Previous studies by KAGRA collaborators [7–9] showed that cooling effectively reduced the coating thermal noise. However, further reduction is necessary not only for KAGRA, but also for future detectors such as the Einstein Telescope [10, 11]. For this purpose, an apparatus for measuring the mechanical loss of the coating at cryogenic temperatures is necessary.

We developed a cryogenic apparatus at University of Toyama, which is affiliated with the KAGRA collaboration, to measure the coating loss [12]. This design is similar to that in a previous study [7]. Herein, we report the details of this apparatus.

2. Outline of the apparatus

We prepared thin sample disks with and without a reflective coating and measured the decay times of the intentionally excited resonant motions of these disks. The mechanical losses of the disks were derived from the measured decay times. The mechanical loss of the coating was calculated from the difference in the mechanical loss between the disks with and without the coating.

The disk was installed in the nodal support system, as shown in Fig. 1. In this system, only the center of the disk was fixed. The electrostatic actuator and transducer were set near the disk, as shown in Fig. 1. The actuator excites the resonant motion, whereas the transducer monitors the resonant vibrations and their decays. The output of the transducer was amplified using a preamplifier and sent to a lock-in amplifier. A logger records the output of the lock-in amplifier.

The nodal support system was placed in a vacuum chamber in a Dewar (Fig. 2). Liquid nitrogen or helium was introduced to cool the chamber. The thermometers and heater were placed in the nodal support system, as shown in Fig. 1 to adjust and observe the temperature.

3. Sample disks

Because the reflective coating is thin (of the order of μm), it is difficult to fabricate only the coating. The coating was then deposited onto the sample disk. The decay times of the resonant

motion of the disks with and without the coating were measured. The difference between the measured decay times corresponds to the mechanical loss in the coating.

The sample disk of our apparatus was a thin circular disk (100 mm in diameter and 0.5 or 1 mm in thickness). Usually, the disk material is the same as that of the mirror used in gravitational wave detectors. In the case of KAGRA, this disk was made of sapphire. However, other materials, such as silicon and fused silica, can be used for measurement purposed. Thicker or smaller diameter disks can be adopted after some improvements to the nodal support system.

4. Nodal support system

Careful design of the mechanical support for oscillators is necessary when we are measuring the decay of the resonant motion of an oscillator. If the mechanical support also vibrates owing to the resonance of the oscillator, the decay time includes the loss in the mechanical support. Nevertheless, we intend to measure only the mechanical loss of the oscillator. A nodal support system was developed to overcome this issue [13]. In the proposed system, only the center of the sample disk was fixed, as shown in Fig. 1. In many modes, the center is the exact node. The vibration of the nodal support system was be minimized. The diameter of the contact area between the nodal support system and disk was 2 mm. A smaller contact area is also feasible.

We measured the loss of the sapphire disk (0.5 mm thickness) without coating to evaluate the loss by the nodal support system. The loss angles (inverse number of the Q-values) of the first and third modes of the disk were approximately 10^{-6} and 10^{-8} , respectively. We assume that these loss angles are limited by the nodal support system because the contact area between the nodal

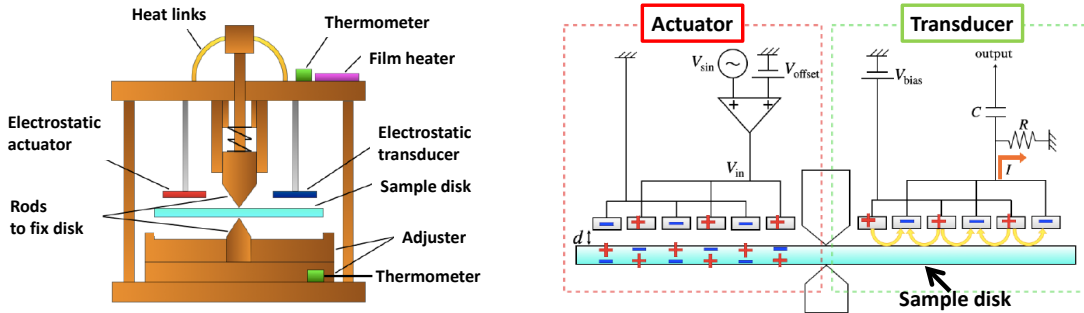


Figure 1: (Left figure) Schematic side view of the nodal support system [12]. Only the center (nodal point) of the sample disk is fixed in the nodal support system [13]. An electrostatic actuator (transducer) to excite the resonant vibration (to monitor the decay of the resonant motion) was installed. Four stainless-steel rods (not shown in this figure) connected the top of the nodal support system to a vacuum chamber. For temperature control, a film heater was fixed on the top of the nodal support system. Two thermometers measured the temperature at the top and bottom of the nodal support system. (Right figure) Schematic side view of the electrostatic actuator and transducer [12] used to excite and observe the resonant motion of the sample disk. Both the actuator and transducer are comb-like electrodes. A high voltage was applied to the electrostatic actuator. The electric field and dielectric polarization exerts a force on the sample disk. A constant voltage was applied on the transducer. When the sample disk moves, the transducer generates electric current owing to transducer capacitance change. The current passed through a resistor. We measured this resistance voltage.

support system and disk is finite. The displacement around the center of the first mode was larger than that of the third mode. This explains why the loss angle of the first mode without the coating is larger. In our previous measurements, the loss angle with the coating was approximately 10^{-5} , which is at least one order of magnitude larger than that without the coating. The coating loss angle was evaluated without difficulty. In future, we anticipate the necessity of certain improvements for measurement of coatings with smaller losses.

The proposed nodal support system is made of copper because it has high thermal conductivity at cryogenic temperatures for a homogeneous temperature. The top side of the nodal support system was connected to a vacuum chamber using four stainless-steel rods, which were the only support to the nodal support system. Because stainless steel has a low thermal conductivity, it is not necessary to provide a large amount of heat to the nodal support system to change its temperature.

5. Electrostatic actuator

Before measuring the decay time of the resonant motion, the resonance must be excited. Therefore, an actuator is required. This actuator must be contactless, or it may introduce a mechanical loss. It should be able to operate in vacuum and at cryogenic temperatures.

An electrostatic actuator, which was a comb-like electrode, was used, as shown in Fig. 1. The electrode was placed above the sample disk. When a voltage (V) is applied to the electrode, force (F) is exerted on the sample disk because of dielectric polarization. This force is proportional to the square of the applied voltage. The applied voltage V can be expressed as:

$$V = V_{\text{offset}} + V_0 \sin(2\pi f_0 t), \quad (1)$$

where V_{offset} is a constant. V_0 and f_0 represent the amplitude and frequency of the sinusoidal voltage, respectively. The force on the sample disk can be obtained as:

$$F \propto V^2 = V_{\text{offset}}^2 + 2V_0 V_{\text{offset}} \sin(2\pi f_0 t) + \frac{V_0^2}{2} [1 - \cos(4\pi f_0 t)]. \quad (2)$$

The second term on the right side of this equation represents the sinusoidal force with frequency f_0 . When this frequency is equal to the resonant frequency, the electrode excites the resonance vibration.

A voltage supply (Matsusada Precision, HJOPS-2B20) was used to apply a constant voltage (V_{offset}), which was approximately a few hundred volts in our measurements. The sinusoidal voltage from the function generator is the input of the Matsusada voltage supply. The output of this power supply is the sum of V_{offset} and the amplified sinusoidal voltage $V_0 \sin(2\pi f_0 t)$. The typical voltage amplitude V_0 is approximately a few hundred volts.

6. Electrostatic transducer

The electrostatic actuator was used to measure resonance decay. The actuator was designed as a comb-like electrode (Fig. 1). A constant voltage (in our measurements, approximately a few hundred volts) was applied to the electrode using a power supply (Matsusada Precision, P4K-80H). For the voltage supply, the electrode acted as a capacitor. The capacitance changed when the sample

disk moved near the electrode. As the voltage applied to this capacitor was constant, the electrode generated an electric current to compensate for the electric charge change in the transducer by the capacitance change. This current passes through the resistance, as shown in Fig. 1. We measured the resistance voltage, which is proportional to the displacement of the sample disk.

However, the drawback of this transducer is its resistance. Because the vibration of the sample disk causes a current in this resistance, it adds to the loss in the sample disk. This loss is proportional to the square of the applied voltage. We investigated the dependence of the disk loss of the measured sample disk on the voltage applied to the transducer. In this study, no voltage dependence was observed. Therefore, in our measurements, we did not consider the loss by the resistance.

7. Amplifier and data logger

As the output of the transducer was small and included noise fluctuations, we used an SR560 (Stanford Research Systems) as a preamplifier and band-pass filter. A band-pass filter removed noise of a frequency range significantly different from the sample disk resonant frequency. The output of the amplifier was sent to a lock-in amplifier (Stanford Research Systems, SR810 DSP). The reference signal was obtained from the function generator for the resonance excitation. The output of the lock-in amplifier was recorded using a logger (HIOKI E.E. CORPORATION, LR8431).

8. Vacuum chamber

The nodal support system, including the sample disk, was installed in a vacuum chamber, as shown in Fig. 2. The chamber was 20 cm in diameter and 35 cm in high. An indium wire was used as a vacuum seal. The upper side of the chamber and the nodal support system were connected to four stainless-steel rods. Above the vacuum chamber, as shown in Fig. 2, several disks were placed as radiation shields.

Dry scroll and turbo-molecular pumps (Agilent Technologies TriScroll 300 Pump and Edwards Vacuum, Inc. STP-iX455) were used. A vacuum gauge was also used (ULVAC, Inc., Pirani Gauge G-TRAN series SPU, multi-ion gauge SH2, and display ISG1) was also used. The pressure was approximately 10^{-2} Pa at room temperature and 10^{-3} Pa below the nitrogen temperature.

9. Dewar

The vacuum chamber and radiation shields described in the previous section were placed in a Dewar, as shown in Fig. 2. After evacuation from the vacuum chamber, liquid nitrogen was poured into the Dewar. Dry nitrogen gas was introduced into the vacuum chamber as the heat exchange gas. The nodal support system and the sample disk were cooled in two days. After cooling, the liquid nitrogen was removed, and liquid helium was poured into the Dewar. Helium gas was introduced into the vacuum chamber. The cooling time is a few hours.

10. Thermometer

Silicon diode thermometers (Lake Shore Cryogenics, Inc., DT-670D-CU-HT) were used in the proposed system. A temperature controller (Lake Shore Cryogenics, Model 336) converted the thermometers outputs into temperatures. It is necessary to measure the sample disk temperature during the measurements. However, we could not place a thermometer on the sample disk because this could result in mechanical loss. Two thermometers were placed on the top and bottom sides of the nodal support system, as shown in Fig. 1. When the temperatures of both thermometers were same, we assumed that it was the temperature of the sample disk. The measurement was recorded when both thermometers reached the same steady-state temperature. Subsequently, we measured the disk loss.

To confirm the above assumption, we conducted the following experiments. Another silicon diode thermometer was placed on the sapphire disk (using glue). This disk was not used for any mechanical loss measurements. It was installed in the nodal support system and cooled. The outputs of the three thermometers were observed. When the two thermometers on the top and bottom sides of the nodal support system recorded the same temperature, the thermometer on the sapphire disk

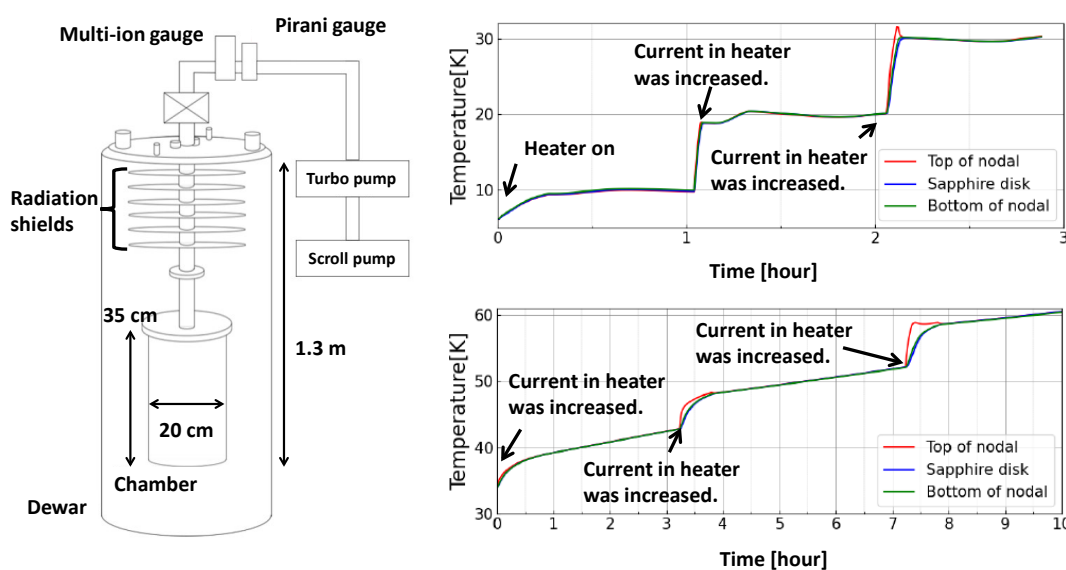


Figure 2: (Left figure) Schematic side view of the vacuum chamber and Dewar [12]. The nodal support system was installed in a vacuum chamber. Above the vacuum chamber, several disks were placed as radiation shields. We used the dry scroll and turbo molecular pumps, and vacuum gauges. This chamber was placed in a Dewar. After evacuation of the vacuum chamber, liquid nitrogen or helium was poured into the Dewar. (Right figure) Temperature of the top and bottom sides of the nodal support system (Top or Bottom of nodal in legend) and (sapphire) sample disk (Sapphire disk in legend) [12]. The turning on of the heater is depicted in the top graph. As seen in the figure, the temperature increases and reaches the steady state. The temperature increases further with an increase in the current passing through the heater. This procedure is repeated. The top (bottom) graph depicts temperature below (above) 30 K. The final temperature is approximately 60 K. With the two thermometers in the nodal support system showing the same temperature, the sapphire disk temperature was determined as the same.

also showed the same temperature, as shown in Fig. 2. This finding supports our hypothesis. It should be noted that the top-side temperature increased immediately after the current in the heater (details are explained in the next section) was increased for short time because the heater was placed on the top side.

Another silicon diode thermometer was placed on top of the vacuum chamber. This thermometer was used to monitor the status of the liquid nitrogen or helium outside the vacuum chamber.

11. Heater

A thin polyimide-film flexible heater (Omega Engineering LLC, KHLVA-0502/5) was placed on the top side of the nodal support system, as shown in Fig. 1. After cooling with liquid helium, the heater was turned on to change the temperature (the temperature controller introduced in the previous section provides current for the heater). We confirmed that the heater could change the temperature between liquid helium and nitrogen.

The heater was placed on the top side of the nodal support system because of its homogeneous temperature. Only the top side of the nodal support system was connected to the vacuum chamber. In case the heater placed on the bottom side, heat flows in the nodal support system, implying a temperature gradient.

12. Measurement

We used our apparatus to measure the loss of the sapphire disks with and without coating. We prepared two types of conventional coatings: the same coating as LIGO and Virgo ($\text{Ti}:\text{Ta}_2\text{O}_5/\text{SiO}_2$) and that of KAGRA ($\text{Ta}_2\text{O}_5/\text{SiO}_2$). Subsequently, we are proceeding with an analysis to derive the coating mechanical loss and thermal noise of KAGRA from the measured data.

Our next measurement involves new coating of LIGO and Virgo (GeO_2). They plan to replace their mirrors with those with the new coating after the current observation (O4), which is expected to continue until the end of 2024. Because the LIGO and Virgo mirrors are at room temperature, we aim to measure the new coating loss at cryogenic temperatures to provide information for the KAGRA decision: regardless of whether KAGRA also adopts this new coating or conventional coating for the KAGRA cooled mirror.

13. Summary

Thermal noise and mechanical loss of mirror coatings are emerging research topic in the field of interferometric gravitational wave detectors. At University of Toyama, we have developed an apparatus to measure the mechanical loss of coatings at cryogenic temperatures. The apparatus was cooled using liquid nitrogen and helium.

We measured the mechanical loss of thin disks with and without coating. We are conducting with an analysis to derive the conventional coating mechanical loss and coating thermal noise amplitude of KAGRA. In future, we aim to investigate potential coating materials for cryogenic interferometers (e.g., KAGRA and Einstein Telescope). Our apparatus should provide clues for reducing the coating loss and thermal noise.

Acknowledgement

We appreciate the valuable support provided by Masatake Ohashi, Takayuki Tomaru, Yoshiki Moriwaki, and Kanta Hattori. The Engineering Machine Shop, Faculty of Engineering, University of Toyama, fabricated the parts of our nodal support system. The Low Temperature Quantum Science Facility at University of Toyama provided the liquid nitrogen and helium for this study. This work was supported by the First Bank of Toyama Scholarship Foundation, and the discretionary budget of the President of University of Toyama.

References

- [1] B.P. Abbott *et al.* (LIGO Scientific Collaboration and Virgo Collaboration), *Phys. Rev. Lett.* **116**, 061102 (2016).
- [2] R. Abbott *et al.* (LIGO Scientific Collaboration, Virgo Collaboration, and KAGRA Collaboration); arXiv:2111.03606 [gr-qc].
- [3] Peter R. Saulson, *Phys. Rev. D* **42**, 2437 (1990).
- [4] Yu. Levin, *Phys. Rev. D* **57**, 659 (1998).
- [5] G. M. Harry *et al.*, *Class. Quantum Grav.* **19**, 897 (2002).
- [6] T. Akutsu *et al.* (KAGRA Collaboration), *Prog. Theor. Exp. Phys.* **2021**, 05A101 (2021).
- [7] K. Yamamoto *et al.*, *Phys. Rev. D* **74**, 022002 (2006).
- [8] E. Hirose *et al.*, *Phys. Rev. D* **90**, 102004 (2014).
- [9] Eiichi Hirose, GariLynn Billingsley, Liyuan Zhang, Hiroaki Yamamoto, Laurent Pinard, Christoph Michel, Danièle Forest, Bill Reichman, and Mark Gross, *Phys. Rev. Applied* **14**, 014021 (2020).
- [10] M Punturo *et al.*, *Class. Quantum Grav.* **27**, 194002 (2010).
- [11] ET steering committee, ET design report update 2020 (<https://apps.et-gw.eu/tds/?content=3&r=17245>).
- [12] Yukino Mori, master thesis (Japanese), University of Toyama (2021).
- [13] K. Numata *et al.*, *Phys. Lett. A* **276**, 37 (2000).